

This is an Open Access document downloaded from ORCA, Cardiff University's institutional repository: <https://orca.cardiff.ac.uk/id/eprint/104577/>

This is the author's version of a work that was submitted to / accepted for publication.

Citation for final published version:

Liu, Shenghua, Zhang, Chunfeng, Zhu, Mengya, He, Qian, Chakhalian, Jak, Liu, Xiaoran, Borisevich, Albina, Wang, Xiaoyong and Xiao, Min 2017. Polar phase transitions in heteroepitaxial stabilized La<sub>0.5</sub>Y<sub>0.5</sub>AlO<sub>3</sub> thin films. *Journal of Physics: Condensed Matter* 29 (40), 405401. 10.1088/1361-648X/aa81ea

Publishers page: <http://dx.doi.org/10.1088/1361-648X/aa81ea>

Please note:

Changes made as a result of publishing processes such as copy-editing, formatting and page numbers may not be reflected in this version. For the definitive version of this publication, please refer to the published source. You are advised to consult the publisher's version if you wish to cite this paper.

This version is being made available in accordance with publisher policies. See <http://orca.cf.ac.uk/policies.html> for usage policies. Copyright and moral rights for publications made available in ORCA are retained by the copyright holders.



**Second Harmonic Generation and Polar Phase Transitions in  
Aluminate Perovskite Thin Films**

Shenghua Liu,<sup>1</sup> Chunfeng Zhang,<sup>1,a)</sup> Mengya Zhu,<sup>1</sup> Qian He,<sup>2</sup> Jak

Chakhalian,<sup>3</sup> Xiaoran Liu,<sup>3,4,b)</sup>

Albina Borisevich,<sup>2</sup> Xiaoyong Wang,<sup>1</sup> and Min Xiao<sup>1,4</sup>

<sup>1</sup>National Laboratory of Solid State Microstructures, School of Physics, and Collaborative Innovation Center of Advanced Microstructures, Nanjing University, Nanjing 210093, China

<sup>2</sup>Materials Science and Technology Division, Oak Ridge National Laboratory, Oak Ridge, Tennessee 37831, USA

<sup>3</sup>Department of Physics and Astronomy, Rutgers University, Piscataway, New Jersey 08854, USA

<sup>4</sup>Department of Physics, University of Arkansas, Fayetteville, Arkansas 72701, USA

## Abstract

We report on the fabrication of epitaxial  $\text{La}_{0.5}\text{Y}_{0.5}\text{AlO}_3$  ultrathin films on (001)  $\text{LaAlO}_3$  substrates. Structural characterization by scanning transmission electron microscopy and X-ray diffraction confirms the high quality of the film with  $a^-b^+c^-$   $\text{AlO}_6$  octahedral tilt pattern. Unlike the nonpolar parent compounds  $\text{LaAlO}_3$  and  $\text{YAlO}_3$ , second harmonic generation measurements on the thin films suggests a nonpolar – polar phase transition at  $T_c$  near 500 K, and a polar – polar phase transition at  $T_a$  near 160 K. By fitting the angular dependence of the second harmonic intensities, we further propose that the two polar structures can be assigned to the  $Pmc2_1$  and  $Pmn2_1$  space group, while the high temperature nonpolar structure belongs to the  $Pbnm$  space group.

Transition metal oxides of  $ABO_3$  with perovskite structure have attracted numerous research attentions for decades because their structural versatility accommodated with a large number of elements at the A- and B- sites leads to exotic properties such as ferromagnetism, superconductivity, colossal magnetoresistance, and metal-insulator transition.<sup>1-3</sup> Polar perovskite compounds without inversion center are of particular interest for the additional symmetry-dependent properties (e.g. piezoelectricity, pyroelectricity, ferroelectricity, and nonlinear optical response), giving rise to materials with multifunctionality.<sup>4</sup> However, except for only a few compounds,<sup>5</sup> it has been generally recognized that most of the perovskite oxides tend to crystallize into nonpolar structures<sup>6-8</sup> with inversion centers preserved by the  $BO_6$  octahedral tilts and rotations accompanied by A-site cation displacement.<sup>8</sup> To overcome this issue, different strategies have been proposed in theory to break the inversion symmetry through chemical doping,<sup>9</sup> epitaxial strain engineering,<sup>10-12</sup> or establishment of artificial superlattices.<sup>13-18</sup> However, it remains an ongoing challenge for experimentalists to search possible candidates of non-centrosymmetric perovskite oxides.

In this letter, we report the discovery of two polar phases in epitaxial  $La_{0.5}Y_{0.5}AlO_3$  (LYAO) thin films grown on (001)  $LaAlO_3$  (LAO) substrate. The quality of the LYAO film has been verified using a combination of characterization methods including scanning transmission electron microscopy (STEM) and synchrotron-based X-ray diffraction. Optical second harmonic generation (SHG) measurements of LYAO film indicate that a nonpolar – polar phase structure takes place at a critical temperature of  $\sim 500$  K, followed by a second polar – polar phase transition at  $\sim 160$  K. Such phase

transitions have never been reported so far in either of the parent constituents (At room temperature, the structure of LAO belongs to space group  $R\bar{3}c$ , while that of YAO belongs to space group  $Pbnm$ ).<sup>19</sup> Detailed analysis on the polarization diagrams of the SHG intensities gives compelling evidences that the point group symmetry of both polar phases is  $mm2$ . We further give discussions on the speculated space group of each phase.

In bulk, both of the pure compounds, LAO and  $YAlO_3$  (YAO) are members of the rare-earth aluminate perovskite, which serve as prototypical materials for scintillators,<sup>20</sup> laser techniques,<sup>21</sup> and high- $\kappa$  dielectrics.<sup>22</sup> It was previously reported that the  $La_{1-x}Y_xAlO_3$  solid solution maintains a single phase with the  $Pbnm$  structure except for  $x = 0.5$ , where the compound is thermodynamically unstable and phase separation occurs.<sup>23</sup> Regarding this, we first investigate whether a single phase  $La_{0.5}Y_{0.5}AlO_3$  can be established in the form of thin film since epitaxial stabilization has been recognized as a powerful tool to realize metastable or unstable phases that are far from the thermodynamical equilibrium in bulk phase diagrams.<sup>24</sup>

Epitaxial LYAO thin films were fabricated on  $5 \times 5 \text{ mm}^2$  (001)-oriented LAO substrates by pulsed laser deposition with a KrF excimer laser operating at  $\lambda = 248 \text{ nm}$ . The ablation frequency was set as 18 Hz, and the substrate was maintained at  $750 \text{ }^\circ\text{C}$  in high vacuum of  $\sim 10^{-6}$  Torr. After growth, the sample was annealed at  $580 \text{ }^\circ\text{C}$  for 30 minutes in an oxygen atmosphere of  $\sim 700$  Torr and then cooled down to room temperature. The entire process of deposition was monitored by *in-situ* reflection-high-energy-electron-diffraction (RHEED). Cross-section STEM images of the film were

taken using the high-angle annular dark-field (HAADF) and bright-field (ABF) methods at Oak Ridge National Laboratory. Synchrotron-based X-ray diffraction (XRD) measurements were performed at beamline BL14B1 of Shanghai Synchrotron Radiation Facility. The wavelength of the incident beam was set at 1.2398 Å. The detailed information about beamline BL14B1 can be found in Ref.<sup>25</sup>.

In order to investigate the crystalline quality of the epitaxial film, STEM images were taken along the pseudocubic  $[110]_{pc}$  axis. The STEM – HAADF images shown in Figure 1(a) clearly demonstrate good crystallinity and uniformity of the LYAO film. As indicated by the yellow dash line, the interface between film and substrate is confirmed to be atomically flat, as the LYAO film appears darker than the LAO substrate due to its lower atomic number on average at the A-site. In addition, the LYAO film is coherently strained to LAO substrate.

To further identify the  $\text{AlO}_6$  octahedral tilt pattern of the film, we took STEM – ABF ~~imaging images on of~~ the highlighted area in LYAO along the pseudocubic  $[110]_{pc}$  axis, shown in Figure 1(b). According to He *et al.*,<sup>26</sup> the shape and symmetry of the oxygen columns in the images projected along the in-plane direction can provide comprehensive information determining the rotation patterns (in-phase or anti-phase) along both in-plane and out-of-plane directions. As displayed in Figure 1(b), the teardrop-like shape of the oxygen columns suggests that in-phase rotation only occurs along one of the in-plane direction, whereas anti-phase rotation takes place along both the other in-plane and the out-of-plane directions<sup>26</sup>. For simplification, we denote it as “ $a^-b^+c^-$ ”, regardless of the magnitude of the rotation angles.

X-ray diffraction (XRD)  $\theta$ - $2\theta$  scans [Figure 1(c)] were performed on the LYAO thin films, as well as a bare LAO substrate. As displayed on the figure, in the vicinity of the sharp peaks of the substrate, only the  $(00l)$  Bragg reflections of the film is observed, excluding the presence of any impurity phase. Besides that, the distinct thickness fringes around each  $(00l)$  reflection further corroborate the flatness of the film surface. The calculated out-of-plane lattice parameter of the LYAO film is 3.880 Å. The total thickness of the film is 9.84 nm as deduced from the distinct fringes, which is in good agreement with values estimated from STEM image.

After confirming the quality of the sample, we next turn to investigate whether the film has a polar structure or possesses any non-polar – polar structural phase transition in a wide temperature range. Optical SHG is an extremely sensitive technique for this purpose, since its strength is directly related to the third-rank polar tensor of a solid.<sup>27-</sup><sup>30</sup> The SH intensities in different coordinate directions can be evaluated by considering a matrix of nonlinear optical susceptibility with 18 elements ( $d_{ij}$ ) having values that are tightly associated to the crystal symmetries.<sup>31</sup> We characterize the space symmetries of the sample by analyzing the measured polarization components of SHG using the reflection geometry [Figure 2(a)] with an angle of incidence  $q = 45^\circ$ . The incident beam was generated from a Ti:Sapphire regenerative amplifier (Libra, Coherent, 100 fs pulses, 1 kHz repetition rate). The samples were mounted on a vacuum cryostat (MicroCryostatHe, Oxford) or a home-built optical chamber filled with oxygen for low-temperature (4-500 K) or high-temperature experiments (300-800 K), respectively. A laser clean filter was placed before the sample to avoid any artifacts caused by optical

surfaces and the output SH signal was filtered by a short-pass filter and detected with a spectrograph (Sp2500i, Princeton Instruments) equipped with a liquid-nitrogen-cooled charge-coupled device. Temperature-dependent SH experiments were performed by gradually increasing the temperature. For polarimetry measurements, we also measured the generated SH signals at two different polarizations, namely, *s*-polarized ( $I_s$ ) and *p*-polarized ( $I_p$ ) SH lights, as set by a linear polarizer before the detector, while the polarization of the incident laser beam is changed by a half-wave plate.

Temperature dependence of SH response was measured from 800 K to 70 K [Figure 2(b)]. As seen, a clear centrosymmetric to non-centrosymmetric phase transition has been detected at a temperature of  $T_c \sim 500$  K, above which the SH intensity diminishes to a minimum background value. The SH intensity reaches a maximal value at  $T \sim 250$  K and gradually decreases as the temperature is lowered. This is similar to the case in Ruddlesden-Popper oxides.<sup>32</sup> The octahedral-rotation-induced noncentrosymmetry causes a temperature-dependent displacement between ions, leading to the drop of nonlinear susceptibility with increasing temperature.<sup>32</sup> In addition, however, an anomaly behavior is detected at  $T_a \sim 160$  K, where the SH intensity suddenly jumps to a higher value, indicative of another possible phase transition.

In Figure 3(a) – 3(d), we show the polarization diagrams of SH radiation of each polarization (red for *s*-polarization and blue for *p*-polarization) measured at 70 K, 150 K, 250 K, and 400 K, all of which are within the non-centrosymmetric region. Information about the nonlinear susceptibility of the film can be obtained through recording the SH intensity as a function of the incident polarization angle of  $\theta$ , with

respect to the  $s$  polarization. Interestingly, the shape of the  $s$ -polarized polar plot has extremely distinct features on either side of the anomaly temperature  $T_a$ , which agrees quite well with the temperature dependent results and provides another evidence that a polar to polar phase transition may take place at  $T_a \sim 160$  K besides the nonpolar to polar phase transition at  $T_c \sim 500$  K.

To shed light on the probable group symmetries of the non-centrosymmetric phases, we performed data fittings on the polar plots of both  $s$ -polarized ( $I_s$ ) and  $p$ -polarized ( $I_p$ ) SH signals. As shown in solid lines in Figure 3(a) – 3(d), results can be reasonably reproduced if fitted based on the orthorhombic  $mm2$  point group symmetry, in which the expression of the nonlinear tensor has the following nonzero coefficients:  $d_{15} = d_{31}$ ,  $d_{32} = d_{24}$  and  $d_{33}$ , where the usual tensor abbreviation subscripts and Klienmann symmetry are applied.<sup>27,31</sup> The resultant SH intensities in our geometry can be therefore derived as ,

$$\begin{aligned} I_s(j) &\propto \left( \frac{d_{33} - d_{15}}{2} \cos^2 j + d_{24} \sin^2 j \right)^2, \\ I_p(j) &\propto (d_{24} \sin 2j)^2 \end{aligned} \quad (1)$$

where  $j$  is the angle of incident polarization with respect to the  $s$  polarization. These give rise to two series of values of the fitting parameters:  $(d_{33}-d_{15})/2 \sim -22.6$ ,  $d_{24} \sim 24.9$  at  $T < T_a$ , whereas  $(d_{33}-d_{15})/2 \sim -39.7$ ,  $d_{24} \sim 2.1$  at  $T > T_a$ .

Combining together the results from STEM imaging and SHG fittings, two conditions need to be satisfied for the determination of the space group symmetries of the polar phases of the film. First, regardless of the magnitude of the tilt angle, the octahedral rotation pattern should be compatible with  $a^- b^+ c^-$ . Second, the space group

should be non-centrosymmetric and belong to the family of  $mm2$  point group. Group theory analysis <sup>6</sup> suggests that there are two most probable space groups for the polar structure,  $Pmc2_1$  (space group No. 26) and  $Pmn2_1$  (space group No. 31). In particular, it has been reported that for both symmetries, the expressions of the SH polar plots have the same form yet only with different values of the tensor elements.<sup>33-35</sup> Therefore we speculate that the anomaly behavior observed on the temperature dependent SH curve at  $T_a \sim 160$  K is a hallmark of polar – polar phase transition between  $Pmc2_1$  and  $Pmn2_1$ . Furthermore, the high temperature ( $T > 500$  K) nonpolar phase is most likely with  $Pbnm$  (space group No. 62) symmetry.

The remaining question is: What is the symmetry of the ground state of LYAO thin film? Although it is difficult to distinguish from SHG fittings, we can think of it from other perspectives. Theoretical calculations have predicted that for bulk  $Pbnm$  perovskites (such as  $\text{CaTiO}_3$  and  $\text{CaMnO}_3$ ) under tensile strain, a  $Pmc2_1$  ground state can be induced and is most stable for intermediate strain, whereas a  $Pmn2_1$  ground state is more energetically favored for larger strain ( $>3.9\%$ ) <sup>10,12,36,37</sup>. In our case, the estimated value of tensile strain is  $\sim 0.93\%$  if we take the average number of YAO ( $a_{\text{YAO}} = 3.72$  Å) and LAO ( $a_{\text{LAO}} = 3.79$  Å) as the LYAO bulk lattice parameter ( $a_0 = 3.755$  Å). As a result, we propose that the ground state is most likely the  $Pmc2_1$  symmetry. This finding is actually in agreement with a recently published work, in which the ground state of 1% tensile-strained  $\text{CaTiO}_3$  films with  $a^-b^+c^-$  octahedral tilt pattern possesses the  $Pmc2_1$  space group symmetry.<sup>38</sup>

In conclusion, high quality LYAO thin film has been fabricated successfully on

LAO substrate for the first time. Characterized by STEM and SHG, it is found that in a wide range of temperature, two structural phase transitions take place in the film: a nonpolar – polar phase transition at 500 K, and another polar – polar phase transition at 160 K. Our results clearly demonstrate the feasibility of establishing new types of noncentrosymmetric structures by means of heteroepitaxial strain engineering and pave another way towards the pursuit of multifunctional materials.

The authors thank J. Young, J. Rondinelli, and L. Bellaiche for fruitful discussions. Also we acknowledge beamline BL14B1 (Shanghai Synchrotron Radiation Facility) for providing the beam time and assistance during experiments. CZ acknowledges Xuewei Wu for his technical assistant. The work at Nanjing is supported by the National Basic Research Program of China (2013CB932903), the National Science Foundation of China (11574140, and 11621091), and Jiangsu Provincial Funds for Distinguished Young Scientists (BK20160019). JC is supported by the Gordon and Betty Moore Foundation's EPiQS Initiative through Grant No. GMBF4534. XL acknowledges the support by the Department of Energy Grant No. DE-SC0012375. [STEM studies \(QH, AYB\) was supported by the Materials Science and Engineering Division of the US DOE Office of Science.](#)

## References

- <sup>1</sup> P. A. Lee, N. Nagaosa, and X. G. Wen, *Rev. Mod. Phys.* **78**, 17 (2006).
- <sup>2</sup> M. B. Salamon and M. Jaime, *Rev. Mod. Phys.* **73**, 583 (2001).
- <sup>3</sup> M. Imada, A. Fujimori, and Y. Tokura, *Rev. Mod. Phys.* **70**, 1039 (1998).
- <sup>4</sup> P. S. Halasyamani and K. R. Poeppelmeier, *Chem. Mater.* **10**, 2753 (1998).
- <sup>5</sup> S. W. Cheong and M. Mostovoy, *Nature Mater.* **6**, 13 (2007).
- <sup>6</sup> H. T. Stokes, E. H. Kisi, D. M. Hatch, and C. J. Howard, *Acta. Crystallogr. B* **58**, 934 (2002).
- <sup>7</sup> C. J. Howard and H. T. Stokes, *Acta. Crystallogr. B* **58**, 565 (2002).
- <sup>8</sup> N. A. Benedek and C. J. Fennie, *J. Phys. Chem. C* **117**, 13339 (2013).
- <sup>9</sup> O. E. Gonzalez-Vazquez, J. C. Wojdel, O. Dieguez, and J. Iniguez, *Phys. Rev. B* **85**, 064119 (2012).
- <sup>10</sup> C. J. Eklund, C. J. Fennie, and K. M. Rabe, *Phys. Rev. B* **79**, 220101 (2009).
- <sup>11</sup> L. Chen, Y. R. Yang, Z. G. Gui, D. Sando, M. Bibes, X. K. Meng, and L. Bellaiche, *Phys. Rev. Lett.* **115**, 267602 (2015).
- <sup>12</sup> E. Bousquet and N. Spaldin, *Phys. Rev. Lett.* **107**, 197603 (2011).
- <sup>13</sup> E. Bousquet, M. Dawber, N. Stucki, C. Lichtensteiger, P. Hermet, S. Gariglio, J. M. Triscone, and P. Ghosez, *Nature* **452**, 732 (2008).
- <sup>14</sup> N. A. Benedek and C. J. Fennie, *Phys. Rev. Lett.* **106**, 107204 (2011).
- <sup>15</sup> J. M. Rondinelli, S. J. May, and J. W. Freeland, *MRS Bull.* **37**, 261 (2012).
- <sup>16</sup> J. M. Rondinelli and C. J. Fennie, *Adv. Mater.* **24**, 1961 (2012).
- <sup>17</sup> S. J. Callori, J. Gabel, D. Su, J. Sinsheimer, M. V. Fernandez-Serra, and M. Dawber, *Phys. Rev. Lett.* **109**, 067601 (2012).
- <sup>18</sup> X. F. Wu, M. Stengel, K. M. Rabe, and D. Vanderbilt, *Phys. Rev. Lett.* **101**, 087601 (2008).
- <sup>19</sup> S. Geller and V. B. Bala, *Acta. Crystallogr.* **9**, 1019 (1956).
- <sup>20</sup> R. L. Wood and W. Hayes, *J. Phys. C* **15**, 7209 (1982).
- <sup>21</sup> I. F. Elder and M. J. P. Payne, *Opt. Commun.* **148**, 265 (1998).
- <sup>22</sup> S. A. Shevlin, A. Curioni, and W. Andreoni, *Phys. Rev. Lett.* **94**, 146401 (2005).
- <sup>23</sup> T. Kyomen and M. Itoh, *J. Therm. Anal. Calorim.* **69**, 813 (2002).
- <sup>24</sup> O. Y. Gorbenko, S. V. Samoilentsov, I. E. Graboy, and A. R. Kaul, *Chem. Mater.* **14**, 4026 (2002).
- <sup>25</sup> T.-Y. Yang, W. Wen, G.-Z. Yin, X.-L. Li, M. Gao, Y.-L. Gu, L. Li, Y. Liu, H. Lin, X.-M. Zhang, B. Zhao, T.-K. Liu, Y.-G. Yang, Z. Li, X.-T. Zhou, and X.-Y. Gao, *Nucl. Sci. Tech.* **26**, 020101 (2015).
- <sup>26</sup> Q. He, R. Ishikawa, A. R. Lupini, L. Qiao, E. J. Moon, O. Ovchinnikov, S. J. May, M. D. Biegalski, and A. Y. Borisevich, *Acs Nano* **9**, 8412 (2015).
- <sup>27</sup> S. A. Denev, T. T. A. Lummen, E. Barnes, A. Kumar, V. Gopalan, and D. J. Green, *J. Am. Ceram. Soc.* **94**, 2699 (2011).
- <sup>28</sup> S. Denev, A. Kumar, M. D. Biegalski, H. W. Jang, C. M. Folkman, A. Vasudevarao, Y. Han, I. M. Reaney, S. Trolier-McKinstry, C. B. Eom, D. G. Schlom, and V. Gopalan, *Phys. Rev. Lett.* **100**, 257601 (2008).
- <sup>29</sup> H. W. Jang, A. Kumar, S. Denev, M. D. Biegalski, P. Maksymovych, C. W. Bark, C. T. Nelson, C. M. Folkman, S. H. Baek, N. Balke, C. M. Brooks, D. A. Tenne, D. G. Schlom, L. Q. Chen, X. Q. Pan, S. V. Kalinin, V. Gopalan, and C. B. Eom, *Phys. Rev. Lett.* **104**, 197601 (2010).
- <sup>30</sup> E. D. Mishina, T. V. Misuryaev, N. E. Sherstyuk, V. V. Lemanov, A. I. Morozov, A. S. Sigov, and T. Rasing, *Phys. Rev. Lett.* **85**, 3664, 3664 (2000).
- <sup>31</sup> R. W. Boyd, *Nonlinear Optics*. (2010).
- <sup>32</sup> H. Akamatsu, K. Fujita, T. Kuge, A. Sen Gupta, A. Togo, S. Lei, F. Xue, G. Stone, J. M. Rondinelli,

- L.-Q. Chen, I. Tanaka, V. Gopalan, and K. Tanaka, *Phys. Rev. Lett.* **112**, 187602 (2014).
- <sup>33</sup> G. Zou, C. Lin, H. Kim, H. Jo, and K. Ok, *Crystals* **6**, 42 (2016).
- <sup>34</sup> X. Jiang, S. Luo, L. Kang, P. Gong, H. Huang, S. Wang, Z. Lin, and C. Chen, *ACS Photonics* **2**, 1183 (2015).
- <sup>35</sup> Y. Yang, X. Jiang, Z. Lin, and Y. Wu, *Crystals* **7**, 95 (2017).
- <sup>36</sup> T. Gunter, E. Bousquet, A. David, P. Boullay, P. Ghosez, W. Prellier, and M. Fiebig, *Phys. Rev. B* **85**, 214120 (2012).
- <sup>37</sup> H. J. Zhao, M. N. Grisolia, Y. R. Yang, J. Iniguez, M. Bibes, X. M. Chen, and L. Bellaiche, *Phys. Rev. B* **92**, 235133 (2015).
- <sup>38</sup> M. D. Biegalski, L. Qiao, Y. J. Gu, A. Mehta, Q. He, Y. Takamura, A. Borisevich, and L. Q. Chen, *Appl. Phys. Lett.* **106**, 162904 (2015).

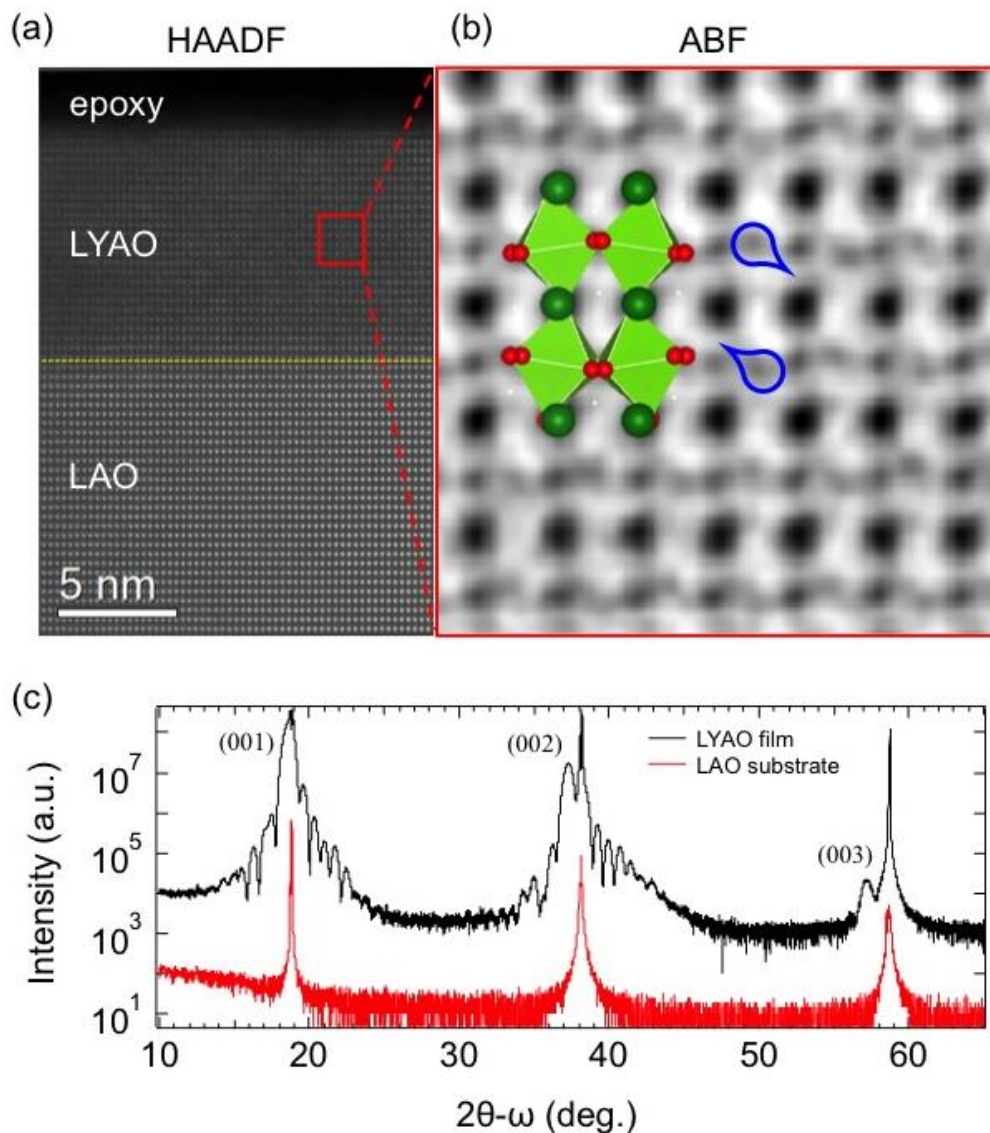


Figure 1. Structural characterizations of the epitaxial LYAO thin film on LAO substrate. (a) STEM-HAADF image of the sample projected along the  $[110]_{pc}$  axis. The other axis is the out-of-plane  $[001]_{pc}$  axis, parallel to the epitaxial growth direction. The interface between film and substrate is indicated by yellow dashed line. (b) ABF image of the highlighted area in LYAO film. Oxygen columns form a teardrop-like shape as outlined in blue, indicating the  $\text{AlO}_6$  rotation pattern as  $a^-b^+c^-$ . (c) Synchrotron-based XRD ( $\lambda = 1.2398 \text{ \AA}$ ) on both the substrate and the sample. The  $(00l)$  Bragg reflections of the film are labeled on the figure.

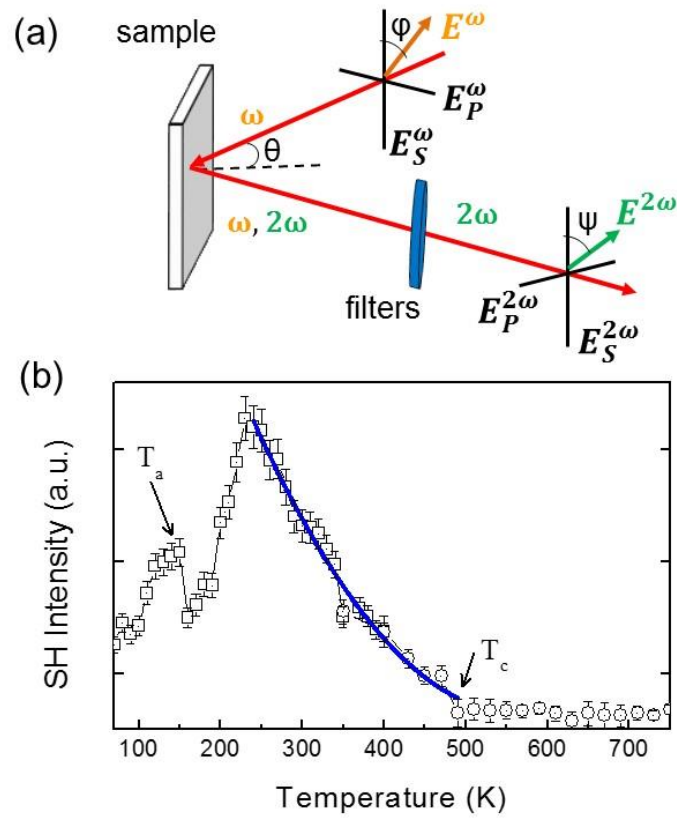


Figure 2. Temperature dependence of the SH intensity. (a) Schematic diagram of the experimental configuration. The fundamental light is incident at  $45^\circ$  to the sample normal, and the SH intensity is recorded at specular reflection. (b) Total SH intensity as a function of temperature. A clear transition at  $T_c \sim 500$  K is observed, whereas an anomaly behavior occurs at  $T_a \sim 160$  K.

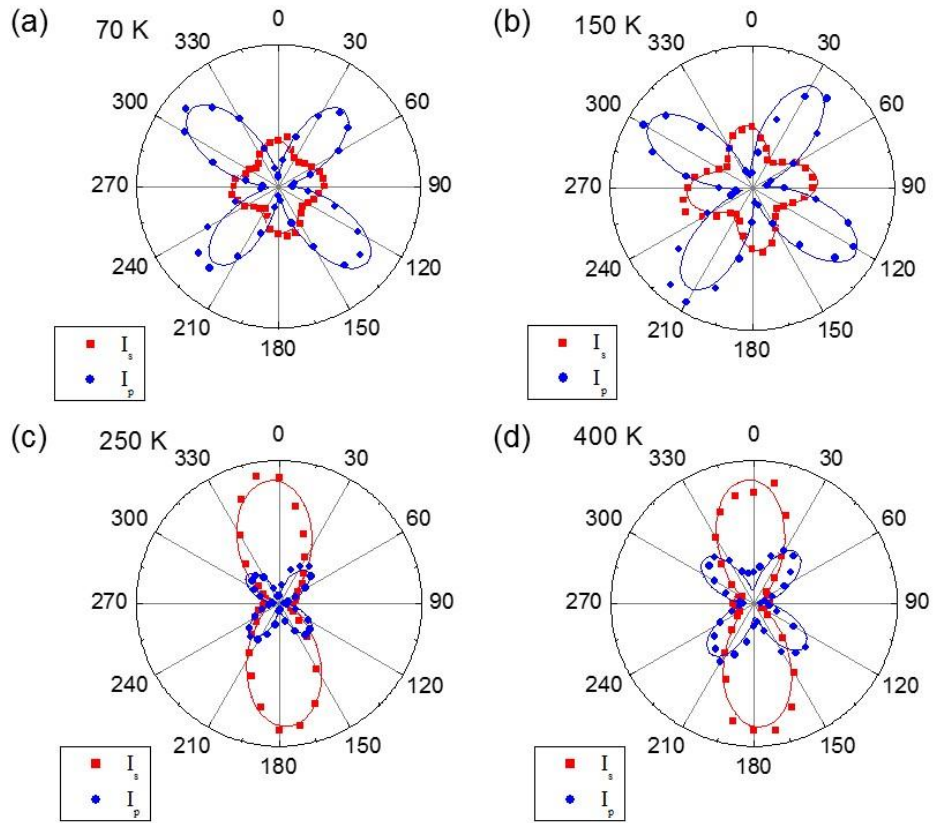


Figure 3. SHG polarization diagrams of LYAO film at different temperatures (red for s-polarization and blue for p-polarization). (a) 70 K; (b) 150 K; (c) 250 K; (d) 400 K. The solid lines are curves fitting using  $mm2$  point group symmetry.